

On the Ternary Silver Alloys

I. The System of Silver, Copper and Zinc

By

Shûzô Ueno

(Received October 23, 1929)

The ternary system of silver, copper and zinc seems not to have been studied hitherto and therefore an attempt was made, as described below, to fill in the blank.

I On the Binary Systems, Copper-Silver, Copper-Zinc and Silver-Zinc

For the copper and silver system, T. Hirose's¹ equilibrium diagram, and for the copper-zinc system, D. Iitsuka's² one, were adopted without any modification. With regard to the silver and zinc system, however, Petrenko's³ latest diagram had to be slightly modified, not in respect of the nature of the equilibrium but in the form of the curves representing the liquidus, solidus or solubility. These must naturally have resulted because of differences in the working conditions. The modifications so tried are given in Fig. 1 in dotted lines, the data used being summarised in Tab. 27.

II Preliminary Experiments

The copper and the silver used as materials were both electrolytically pure, while the zinc was not so pure, yet of Merck's best quality. In order to avoid changes in the composition by volatilization, the silver was first fused under molten sodium chloride in a porcelain

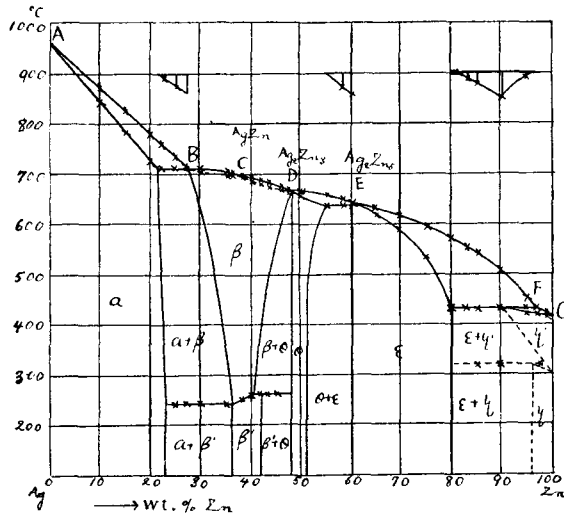
1 Report of the Imperial Mint, Osaka, No. 1, 1 (1927)

2 These memoirs, VIII, 180 (1925); Metallkunde 19, 396 (1927)

3 Zeits. Anorg. C. 165, 297 (1927)

crucible, and while it was kept at temperatures a little higher than its melting point, the zinc and the copper were thrown in piece by piece and well stirred. The alloys thus prepared generally underwent

Fig. 1



a very slight loss and were found on analysis to contain 0.3%—0.5% Zn short of the given compositions. The experiments were made on the alloys as shown in Table 1.

Tab. 1

Metals taken in %		Metals analysed in %		Loss of Zn in %
Cu	Ag	Cu	Ag	
70	20	70.11	20.20	0.31
40	50	40.09	50.25	0.34
20	70	20.06	70.22	0.28
10	80	10.02	80.16	0.18
70	10	70.31	10.04	0.35
10	70	10.04	70.36	0.40
60	10	60.38	10.04	0.42
50	20	50.20	20.08	0.28
40	30	40.22	30.17	0.39
30	40	30.20	40.28	0.48
20	50	27.15	50.37	0.52
10	60	10.04	60.21	0.25
55	5	55.30	5.03	0.33
50	10	50.29	10.06	0.35

Through the microscopical examination of these alloys, the author came roughly to the conception that there is no field consisting of three phases, but that the β solid solution of the Cu-Zn system unites with β of the Ag-Zn system, and ϵ of the Cu-Zn system with ϵ of the Ag-Zn system, so that there are formed two wide homogeneous fields, secluded by which there would remain three heterogeneous fields in the triangular base. Such a conception was confirmed by further investigation, as will be described later.

Tab. 1 (continued)

Metals taken in %		Metals Analysed in %		Loss of Zn in %
Cu	Ag	Cu	Ag	
40	20	40.26	20.14	0.40
25	35	25.23	35.19	0.42
15	45	15.19	45.28	0.47
5	55	5.09	55.46	0.55
10	40	10.04	40.16	0.20
35	15	35.13	15.05	0.18
25	25	25.20	25.18	0.38
15	30	15.09	30.18	0.27
10	35	10.06	35.23	0.29
5	25	5.04	25.23	0.27
10	20	10.12	20.23	0.35
15	10	15.17	10.11	0.28
10	10	10.13	10.17	0.30
10	15	10.14	15.21	0.35
5	5	5.17	5.25	0.42
5	70	5.03	70.28	0.31
"	"	5.04	70.28	0.32
"	"	5.05	70.33	0.38
"	"	5.07	70.26	0.33
"	"	5.03	70.31	0.34
"	"	5.11	70.25	0.36
"	"	5.05	70.16	0.21
"	"	5.07	70.25	0.32
"	"	5.02	70.33	0.35
"	"	5.09	70.28	0.37
"	"	5.15	70.18	0.33

With these results, the sectional diagram, Fig. 2, is plotted, where the liquidus AC represents the primary separation of a , BC that of a , and in the solidus $ad'Cb'b$ ad' stands for the complete crystallization of a , bb' that of a , and $a'C$ and $b'C$ that of the binary eutectic ($a+a$).

The binary eutectic point C lies at 10% Zn, 63% Ag and 27% Cu, where the three phases a , a and the melt form a monovariant system.

The solid phases with the composition marked with the black spots were annealed for a few hours at the corresponding temperatures and quenched, and were then microscopically tested for their structures,

III Cooling Curves

Each alloy weighed 20 gms, to which some more zinc was added to compensate for the loss through volatilization. No chemical analysis was made except for those given in Tab. I. All the alloys were directly fused in an electric furnace and thermally analysed by means of a Pt-Pt. Rh couple carefully calibrated.

IV Sectional-Diagrams

In order to establish the ternary equilibrium diagram, it was necessary first to get a number of sectional diagrams. The results of investigation are given below.

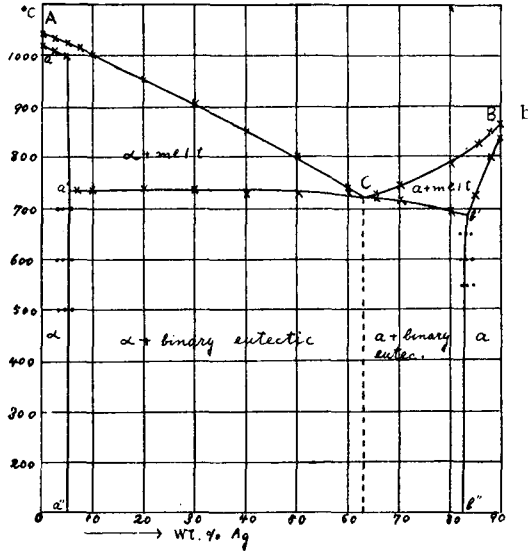
1 10% Zn-Section

The alloys of the compositions given in Tab. 2 were selected along the sectional line of 10% Zn. They were thermally analysed, the results of the analysis being given in Tab. 2.

Tab. 2

Alloy No.	Wt.-%			°C	
	Ag	Cu	Zn	Liqui- dus	Soli- dus
1	—	90	10	1040	1020
2	2	88	"	1035	1005
3	5	85	"	1022	999
4	7	83	"	1013	733
5	10	80	"	999	734
6	20	70	"	948	735
7	30	60	"	900	735
8	40	50	"	845	728
9	50	40	"	795	727
10	60	30	"	735	725
11	65	25	"	728	720
12	70	20	"	740	714
13	80	10	"	785	695
14	85	5	"	825	725
15	88	2	"	850	800
16	90	—	"	865	845

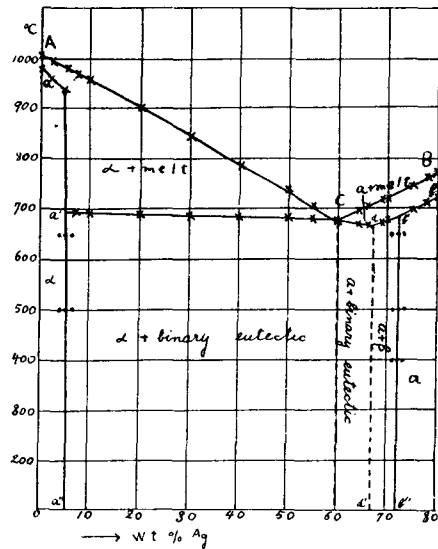
Fig. 2



Tab. 3

Alloy No.	Wt.-%			°C	
	Ag	Cu	Zn	Liqui- dus	Soli- dus
17	—	80	20	1000	978
18	2	78	"	990	960
19	5	75	"	975	945
20	7	73	"	966	690
21	10	70	"	952	692
22	20	60	"	900	693
23	30	50	"	844	689
24	40	40	"	790	684
25	50	30	"	742	688
26	55	25	"	710	686
27	60	20	"	681	680
28	64	16	"	698	676
29	66	14	"	706	672
30	69	11	"	712	673
31	70	10	"	720	680
32	75	5	"	745	700
33	78	2	"	760	715
34	80	—	"	772	725

Fig. 3



and in accordance with those results the solubility curves were drawn as shown in the same diagram.

2 20% Zn-Section

The alloys shown in Tab. 3 were used for the establishment of the 20% Zn-sectional diagram. The results of the thermal analysis are given with them in the same Table. The sectional diagram, Fig. 3, is drawn from the data just given.

The liquidus ACB has the same meaning as that given in the 10% Zn sectional diagram. The solidus $aa'Cdb'b$ differs however from it in this:— 1) Cd represents the crystallization of the binary eutectic $a + \alpha$, 2) db' represents the crystallization of the binary complex $a + \beta$. The binary eutectic point C lies at 20% Zn, 60% Ag and 20% Cu, where the three phases α , a and the melt are in equilibrium.

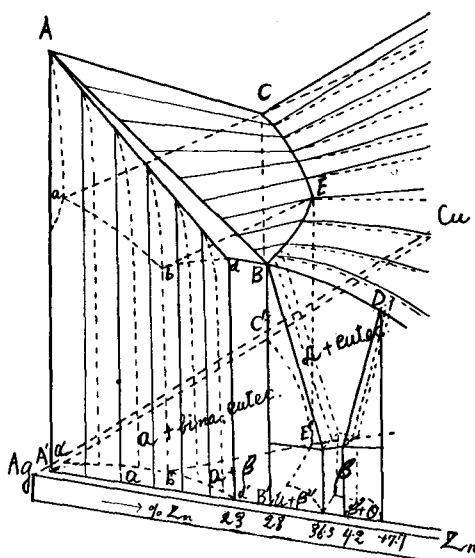
3 The Silver Corner containing over 70% Silver

The liquidus and the solidus were first determined, and the solubility curves were then drawn according to the quenched structures.

For the purpose of quenching, 30 gms. of each of the required alloys were prepared, cut in pieces, and annealed for a few hours at definite temperatures, at which each alloy was thrown into water. The temperatures of quenching and the corresponding structures are here omitted in order to make the paper not too voluminous, but according to these data, the silver-corner diagram was drawn as shown in Fig. 4.

Though the homogeneous solid solution at the silver side in the silver-copper system shows a tendency for the eutectic to be segregated by the low temperature annealing, this property is so markedly lessened by the addition of the zinc that the ternary alloys containing over 10% Zn no longer show any tendency towards segregation, however long they may be annealed. The temperature of the binary eutectic of silver and copper is depressed from 776° to

Fig. 4



670° in relation to the amount of zinc added. This relation is represented by the curve CE along which the equilibrium of the three phases a , α and the melt is established.

Now turning to the Ag-Zn system, these metals form a series of silver-rich solid solutions a , in which the copper comes to be dissolved to the amount of 7.7% and forms a series of ternary solid solutions also named a . The binary solid solution a reacts also with the melt at 710° along the horizontal line dB , where the binary peritectic reaction, $\text{Liq} + a \rightleftharpoons \beta$, comes to proceed. This reaction is prolonged to the ternary melt, the temperature of which is depressed to 670° with the increase in the copper added. This relation is represented by the curve BE along which a , β and the melt are in equilibrium. The binary eutectic curve CE and the peritectical line BE vanish at a point E , which was found to lie at 61.7% Ag, 15% Cu and 23.3% Zn by combining a point d in the 20% Zn-section and another point d in 70% Ag-section, as will be described afterwards. The curve Eb is a boundary line between a surface $abECa$ showing the binary eutectic reaction and a surface $EbdBE$ showing the binary peritectic reaction.

The microstructure of the binary eutectic field is easily to be distinguished from that of the binary peritectic field in so far as they are mutually remote from the line bE Cp. Photo 4: ($a + \text{Eutec.}$) and Photo 10: ($a + \beta$). Closer to the curve bE , both structures become so much more similar, that it is practically impossible for them to be discriminated, although cooling curves given in the 20% Zn-section show clearly the existence of such differences. The fields recognizable at ordinary temperatures are therefore as follows:

- 1 $a'b'd'A'a'$: the structure being a
- 2 $a'b'E'C'a'$: the structure being $a + \text{eutec.}$
- 3 $b'E'B'd'b'$: the structure being $a + \beta$

4 30% Zn-Section

The alloys shown in Tab. 4 were used for the investigation of the 30% Zn-section, the results of which are given in the same table. The sectional diagram, Fig. 5, is drawn on the basis of the data just given.

The liquidus consists of two parts, of which AC stands for the separation of a , and BC for that of β . The solidus consists also of several branches, of which: 1) aa' stands for the complete cry-

Tab. 4

Alloy No.	Wt.-%			°C			
	Ag	Cu	Zn	Liquidus	Solidus	Peritectic	Transformation
35	—	70	30	948	913	—	—
36	2	68	„	936	900	—	—
37	5	65	„	920	680	—	—
38	10	60	„	896	676	—	—
39	20	50	„	835	674	—	—
40	24	46	„	815	673	—	—
41	25	45	„	810	671	—	—
42	27	43	„	800	—	775	—
43	30	40	„	780	—	765	—
44	35	35	„	750	—	743	—
45	40	30	„	725	722	—	—
46	50	20	„	684	675	—	—
47	60	10	„	680	675	—	—
48	65	5	„	690	682	—	241
49	70	—	„	709	705	—	242

stallization of α ; 2) $a'b'$ stands for that of the binary eutectic $a + \alpha$; 3) bc stands for that of the binary complex $a + \beta$ due to the peritectic reaction $Liq. + \alpha \rightleftharpoons Liq. + \beta$ in the Cu-Zn system.

The segregation of α from β takes place along the curve $c'd$ due to the decrease in solubility on the temperature being lowered. The curve gh corresponds to the transformation of β into β' , which is perceptible through the cooling

curves obtained with the alloys containing below 5% Cu.

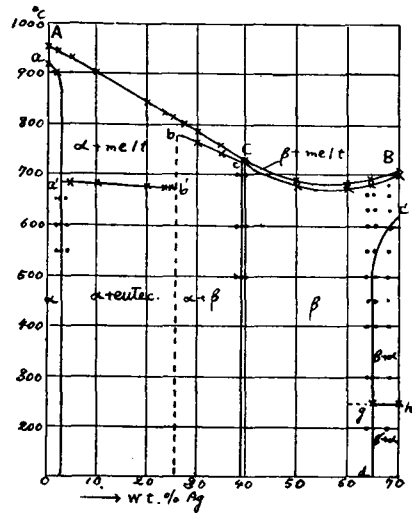
5 35% Zn-Section

The alloys given in Tab. 5 were used for the investigation of the 35% Zn-section, the results of which are given in the column following the composition of the alloys in the same table.

The sectional diagram, Fig. 6, is drawn on the basis of these data.

The binary peritectic reaction, $Liq. + \alpha \rightleftharpoons Liq. + \beta$, in the copper-zinc system is continued in the ternary system, in consequence of which β is separated along the curve aC , the point C being at 17% Ag, 35% Zn and 48% Cu, where the three phases α , β and the melt are in equilibrium. The curve $a'a''$ shows the solubility of β in α as was determined by the quenching method.

Fig. 5



Tab. 5

Alloy No.	Wt.-%			°C			
	Ag	Cu	Zn	Liquidus	Solidus	Peritectic	Transformation
50	—	65	35	910	—	891	—
51	5	60	„	885	—	870	—
52	10	55	„	860	—	850	—
53	15	50	„	833	828	829	—
54	20	45	„	808	800	—	—
55	30	35	„	760	751	—	—
56	40	25	„	710	700	—	—
57	50	15	„	684	675	—	—
58	60	5	„	689	681	—	—
59	63	2	„	697	689	—	245
60	65	—	„	705	700	—	240

6 40% Zn-Section

The alloys used are given in Tab. 6, in which the results of the thermal analysis are co-tabulated.

The sectional diagram drawn on the basis of these data is shown in Fig. 7, where the dotted lines cd and $c'd'$ are provisionally drawn to show the transformation, $\beta \rightarrow \beta_1 \rightarrow \beta_2$ in the binary Cu-Zn system,

though no such breaks could be observed in the author's cooling curves.

7 45% Zn-Section and 50% Zn-Section

The compositions of the alloys and their thermal data with regard to these two sections are given in Tables 7 and 8.

The sectional diagrams, Figs. 8 and 9 are drawn on the basis of these data.

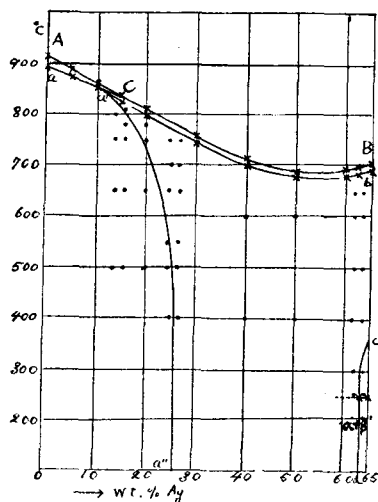
The changes in solubility on the temperatures being lowered are represented by cd' with respect to the segregation of θ from β in 45% Zn-section and $a'SS'$ with respect to that of γ from β in 50% Zn-section.

8 55% Zn-Section

The alloys used and their thermal data are given in Tab. 9, on the basis of which the sectional diagram, Fig. 10, is drawn.

The liquidus AC and the solidus aS represent the separation of β , while the liquidus BC and the solidus bS show that of γ . The solidus bc is due to the peritectic reaction, $Liq. + \theta \rightarrow \epsilon$, belonging to the Ag-

Fig. 6



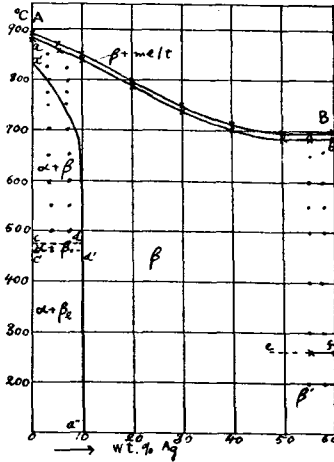
Tab. 6

Alloy No.	Wt.-%			°C			
	Ag	Cu	Zn	Liquidus	Solidus	Transformation I	Transformation 2
61	—	60	40	890	884	460?	—
62	5	55	„	870	862	—	—
63	10	50	„	849	842	—	—
64	20	40	„	797	788	—	—
65	30	30	„	749	739	—	—
96	40	20	„	705	697	—	—
67	50	10	„	684	678	—	—
68	55	5	„	689	781	264	—
86	60	—	„	695	585	260	—

Zn system, while the curve *SC* refers to the separation of γ due to the peritectic reaction, $\text{Liq.} + \beta \rightleftharpoons \text{Liq.} + \gamma$, in the Cu-Zn system. The solid solution θ becomes identical to γ when the amount of copper attains a definite proportion which is however not

Fig 7.

easily to be determined. The changes in solubility on the temperatures being lowered are represented by $\alpha'S$ with respect to the separation of γ from β and $S'S'$ with respect to that of β from γ . The saturating-point of γ in β is shown by *S*, a point with the concentration of 5% Ag, 55% Zn and 40% Cu.



Tab. 7

Alloy No.	Wt.-%			°C			
	Ag	Cu	Zn	Liquidus	Solidus	Transformation I	Transformation 2
70	—	55	45	883	873	471	460?
71	5	50	„	860	852	—	—
72	10	45	„	837	827	—	—
73	21	35	„	785	777	—	—
74	30	25	„	733	724	—	—
75	40	15	„	697	687	—	—
76	50	5	„	678	672	—	—
77	52	3	„	677	671	263	—
78	55	—	„	679	670	261	—

Tab. 8

Alloy No.	Wt.-%			°C			
	Ag	Cu	Zn	Liquidus	Solidus	Transformation 1	Transformation 2
79	—	50	50	868	862	471	460
80	5	45	''	845	833	—	—
81	10	40	''	820	805	—	—
82	20	30	''	772	756	—	—
83	30	20	''	716	705	—	—
84	40	10	''	681	673	—	—
85	50	—	''	668	656	—	—

Fig. 8

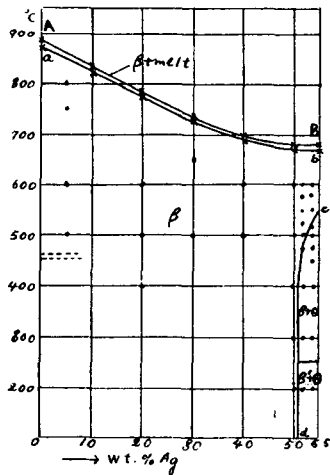
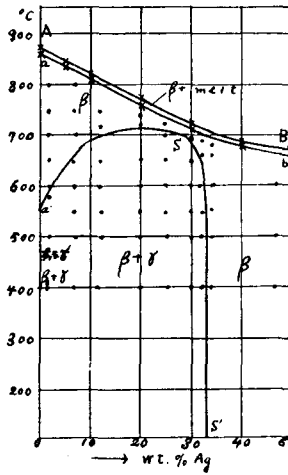


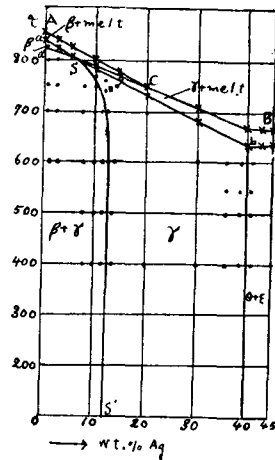
Fig. 9



Tab. 9

Alloy No.	Wt.-%			°C		
	Ag	Cu	Zn	Liquidus	Solidus	Peritectic
86	—	45	55	853	841	—
87	2	43	''	831	825	—
88	5	40	''	825	808	—
89	10	35	''	800	783	790
90	15	30	''	775	757	762
91	20	25	''	750	735	745
92	23	22	''	735	717	732
93	30	15	''	703	680	—
94	40	5	''	662	630	—
95	43	2	''	657	633	—
96	45	—	''	655	635	—

Fig. 10



9 The Equilibrium-Diagram for 0-55% Zn including the Copper-rich Side

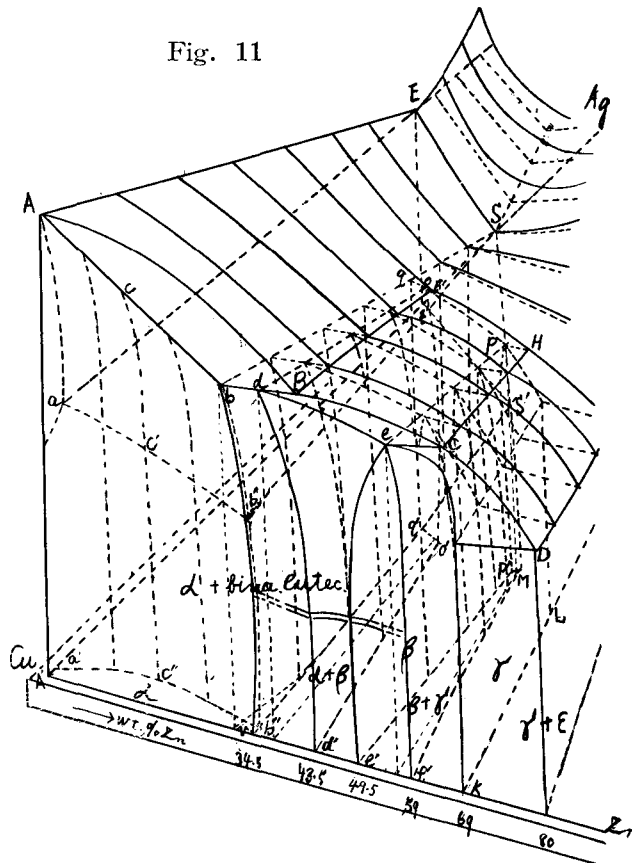
The thermal analysis as well as the quenching method was used in order to establish this equilibrium, as a results of which the diagram, Fig. 11, was drawn.

The surface $ABSEA$ represents the liquidus of a and the surface $ab'SEa$ the solidus of a binary eutectic $a+a$.

The copper-rich solid solution in the Cu-Zn system dissolves silver to the extent of 5.5% and produces a ternary solid solution a , the solidus of which is represented by the surface $Acbb'c'aA$.

The horizontal line bB stands for the peritectic reaction, $Liq. + a \rightleftharpoons Liq. + \beta$, at 890° in the Cu-Zn system. The temperature of

Fig. 11



the reaction is depressed on the addition of silver, as it finally attains the position of a point F on a curve BF representing the peritectical reaction due to the Cu-Zn system, as the following equation shows:-
 $Liq. + a \rightleftharpoons Liq. + \beta$. This line vanishes at about 38% Ag, 32% Zn and 30% Cu, where β dissolves a completely, as the surface $bB-Fg$ shows.

The surface $dd'o'd$ is a solubility surface of β in a originating from the curve

dd' in the Cu-Zn system. This fact is confirmed by the following experiment:-An alloy of 5% Ag, 40% Zn and 55% Cu, quenched at 600° , was seen to have a bistructure consisting of $a + \beta$ (Photo 13),

while, when quenched at 825° , it becomes homogeneous: (Photo 14). The solid solution β becomes saturated with α along the curve do , which corresponds to the point d in the Cu-Zn system. The liquidus of β is shown by $SBCH$ and the solidus by $SqodeP$, but they extend so much further that they can not completely be drawn within the space occupied by Fig. 11.

The horizontal line cC represents the peritectic reaction in the Cu-Zn system at 830° : $\text{Liq.} + \beta \rightleftharpoons \text{Liq.} + \gamma$. Its temperature falls on the silver being increased, as shown by the curve CH . This peritectical line vanishes at about 36% Ag, 13% Cu and 51% Zn, where all comes to be dissolved in β , as the surface $ccHP$ shows. The γ , which is produced by this reaction, solidifies at the surface $eKLPc$: Cp. Photo 22. The solid solution β segregates γ along the surface $cc'p'pc$ on the temperature being lowered, due to the decrease in solubility. An alloy with 2% Ag, 55% Zn and 43% Cu, when quenched at 600° shows the structure $\beta + \gamma$: Cp. Photo 20. When quenched however at 820° , it turns homogeneous ($\neg\gamma$), as may be seen from Photo 21. The β is segregated from γ along the surface $efMPe$ due to the decrease in solubility on the temperature being lowered. Thus, we get in this corner six fields at room temperature:

- 1 $a'C''b''qA'a'$: the structure being α
- 2 $a'c''b''S'E'a'$: the structure being $\alpha + \text{eutec.}$
- 3 $vb''d'd'o'q'b''V$: the structure being $\alpha + \beta$
- 4 $S'q'd'd'e'P'$: the structure being β
- 5 $e'P'M'e'$: the structure being $\beta + \gamma$
- 6 $M'f'KL$: the structure being γ

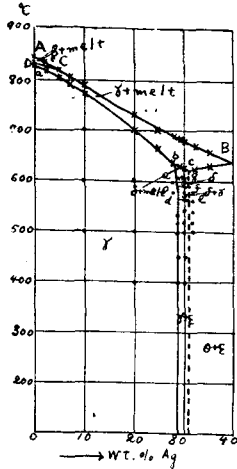
10 60% Zn-Section

The composition of the alloys used and their thermal data are given in Tab. 10.

Tab. 10

Alloy No.	Wt.-%			°C				
	Ag	Cu	Zn	Liquidus	Solidus	Peritectic	Separation of ϵ or γ from δ	Eutectoidal transformation
97	—	40	60	838	825	830	—	—
98	2	38	''	830	817	826	—	—
99	5	35	''	815	801	808	—	—
100	7	33	''	803	788	—	—	—
101	10	30	''	785	777	—	—	—
102	20	20	''	729	705	—	—	—
103	25	15	''	700	660	—	—	—
104	28	12	''	685	635	—	—	—
105	29	11	''	680	611	627	—	—
106	30	10	''	675	610	623	590?	562?
107	32	8	''	664	—	622	—	—
108	35	5	''	650	628	—	—	—
109	40	—	''	637	—	636	—	—

The sectional diagram drawn on the basis of the data is given in Fig. 12, where the liquidus AC stands for the separation of β , and BC for that of γ . There take place two binary peritectic reactions belonging to the Cu-Zn system, one of which is $\text{Liq.} + \beta \rightleftharpoons \text{Liq.} + \gamma$, and as its result γ is separated along the curve DC , while the other is $\text{Liq.} + \gamma \rightleftharpoons \text{Liq.} + \delta$, and as its result δ is separated along the curve bc . There takes place also in the Ag-Zn system a peritectic reaction:— $\text{Liq.} + \theta \rightleftharpoons \epsilon$, ϵ of which is separated along the curve Bc . The crystallization of γ takes place along the solidus ab , that of δ along $a'g$ and that of the binary complex $\gamma + \epsilon$ due to the binary peritectic reaction, $\text{Liq.} + \theta \rightleftharpoons \epsilon$, in the Ag-Zn system along Bc . The curve of corresponds to the separation of γ from δ , and the curve dc shows the eutectoidal transformation, $\delta \rightleftharpoons \gamma + \epsilon$, in the Cu-Zn system.



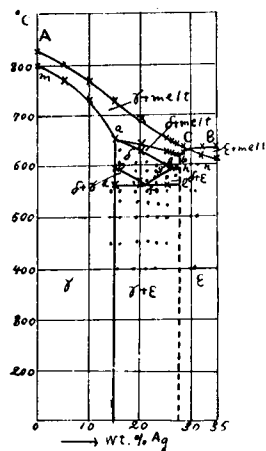
11 65% Zn-Section

The alloys used and their thermal data are given in Tab. 11.
Tab. 11

Alloy No.	Wt.-%			°C					
	Ag	Cu	Zn	Liquidus	Solidus	Peritectic 1	Peritectic 2	Separation of γ or ϵ from δ	Eutectoidal transformation
110	—	35	65	827	800	—	—	—	—
111	5	30	„	800	770	—	—	—	—
112	10	25	„	768	730	—	—	—	—
113	15	20	„	730	—	650	—	595	560
114	20	15	„	694	627	640	—	570?	561
115	22.5	12.5	„	675	615?	635	—	570?	561
116	25	10	„	659	600	623	—	—	560
117	26	9	„	650	—	622	595	—	—
118	27	8	„	642	—	621	595	—	—
119	28.5	6.5	„	635	—	624	—	—	—
120	30	5	„	630	627	—	—	—	—
121	32	3	„	633	612	—	—	—	—
122	35	—	„	633	611	—	—	—	—

On the basis of these data, the sectional diagram, Fig. 13, is drawn, in which the liquidus AC stands for the separation of γ and BC for

Fig. 13



that of ϵ . The solidus $maghbcn$ consists of several branches, of which ma stands for the solidification of γ ; ag for that of δ ; gh for the binary peritectic reaction, $\text{Liq.} + \delta \rightleftharpoons \epsilon$, in the Cu-Zn system; Cn for the solidification of ϵ ; and bc for that of the binary complex $\gamma + \epsilon$ due to the binary peritectic reaction, $\text{Liq.} + \theta \rightleftharpoons \epsilon$, in the Ag-Zn system. The curve de results from the eutectoidal transformation, $\delta \rightleftharpoons \gamma + \epsilon$, in the Cu-Zn system. The curve of corresponds to the separation of γ and the curve gf to that of ϵ from δ . The three phases γ , δ and ϵ are in equilibrium at the point f .

12. 70% Zn-Section

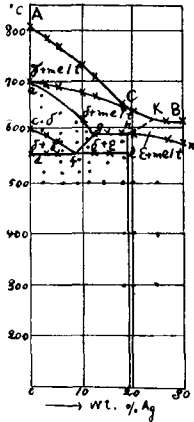
The alloys taken and their thermal data are given in Tab. 12.

Tab 12

Alloy No.	Wt.-%			°C					
	Ag	Cu	Zn	Liquidus	Solidus	Peritectic 1	Peritectic 2	Separation of γ or ϵ from δ	Eutectoidal transformation
123	—	30	70	800	—	695	—	600?	556
124	3	27	„	780	677	690	—	587	557
125	5	25	„	765	665	682	—	580?	558
126	10	20	„	730	625	670	—	570	559
127	12.5	17.5	„	710	597	665	—	594	560
128	15	15	„	685	—	658	595	—	560
129	18	12	„	657	—	650	596	—	—
130	20	10	„	637	—	—	594	—	—
131	22.5	7.5	„	627	596	—	—	—	—
132	25	5	„	619	591	—	—	—	—
133	27.5	2.5	„	619	590	—	—	—	—
134	30	—	„	619	583	—	—	—	—

The sectional diagram is drawn in Fig. 14. It is quite similar to the previous diagram, except the part ghk , along which ϵ is separated due to the reaction, $\text{Liq.} + \delta \rightleftharpoons \text{Liq.} + \epsilon$, in the Cu-Zn system. The data from the cooling curves were however not sufficient to fix the part hk , and therefore it is now provisionally shown with dotted lines.

Fig. 14



13 75% Zn-Section

The alloys taken and their thermal data are given in Tab. 13, and the sectional diagram drawn on the basis of these data is given in Fig. 15.

The liquidus *AC* corresponds to the separation of γ , *CD* to that of δ , and *BD* to that of ϵ . The solidus consists of two branches of which *af* stands for δ and *gn* for ϵ . The δ is separated along the curve *aC* due to the binary peritectic reaction, $Liq. + \gamma \rightleftharpoons Liq. + \delta$, in the Cu-Zn system. The point *C* lies at 10% Ag, 75% Zn and 15% Cu, where the three phases γ , δ and the melt are in equilibrium. Along the curve *gD*, ϵ is separated due to the binary peritectic reaction, $Liq. + \delta$

Tab. 13

Alloy No.	Wt.-%			°C					
	Ag	Cu	Zn	Liquidus	Solidus	Peritectic 1	Peritectic 2	Separation of ϵ from δ	Eutectoidal transformation
135	—	25	75	750	650	695	—	575?	556
136	2	23	„	742	615	691	—	575	556
137	5	20	„	714	600	683	—	576	557
138	7.5	17.5	„	697	598	680	—	—	558
139	10	15	„	675	593	672	595	—	—
140	15	10	„	630	585	—	595	—	—
141	20	5	„	592	570	—	—	—	—
142	25	—	„	597	536	—	—	—	—

$\rightleftharpoons Liq. + \epsilon$, in the Cu-Zn system. The point *C* lies at 18% Ag, 75% Zn and 7% Cu, where the three phases γ , ϵ and the melt are in equilibrium. The curve *fg* shows the separation of ϵ from δ , while the *dc* has the same meaning as given in the previous section.

14 80% Zn-Section

The alloys used and the thermal data are given in Tab. 14, and the sectional diagram is shown in Fig. 16.

This section is so similar to the previous one that it needs no more explanation.

Fig. 15

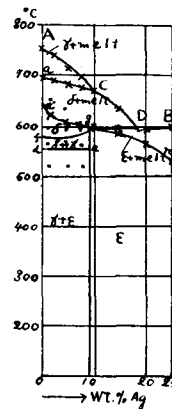
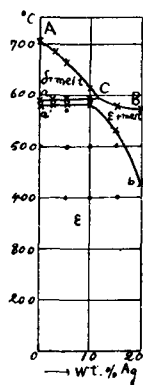


Fig. 16



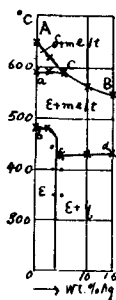
Tab. 14

Alloy No.	Wt.-%			°C		
	Ag	Cu	Zn	Liquidus	Solidus	Peritectic
143	—	20	80	700	580	590
144	2.5	17.5	''	685	581	591
145	5	15	''	660	584	593
146	10	10	''	610	585	596
147	15	5	''	575	532	—
148	20	—	''	570	435	—

15 98% Zn-Section

The alloys taken and the thermal data are given in Tab. 15, and the sectional diagram is given in Fig. 17.

Fig. 17



Tab. 15

Alloy No.	Wt.-%			°C			
	Ag	Cu	Zn	Liquidus	Solidus	Peritectic 1	Peritectic 2
149	—	15	85	647	480	590	—
150	2.5	12.5	''	620	480	592	—
151	5	10	''	595	—	592	426
152	10	5	''	557	—	—	428
153	15	—	''	544	—	—	480

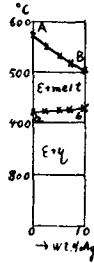
This section differs from the previous only in the part bcd , where ϵ solidifies along bc and η is separated along cd due to the binary peritectic reaction, $\text{Liq.} + \epsilon \rightleftharpoons \eta$, in the Cu-Zn system.

16 90% Zn-Section

The alloys taken and the thermal data are given in Tab. 16, and the sectional diagram is as shown in Fig. 18.

The curve AB represents the liquidus of ϵ , and ab the curve of separation of η' due to the binary peritectic reaction: $\text{Liq.} + \epsilon \rightleftharpoons \eta'$.

Fig. 18



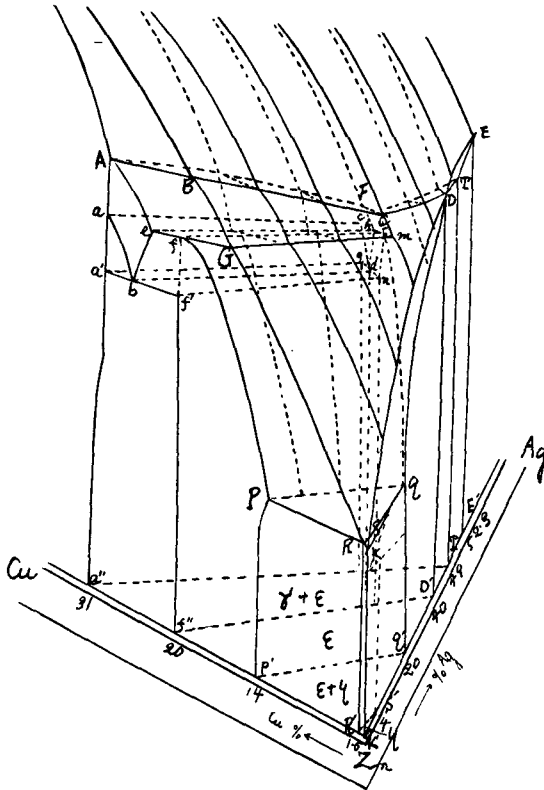
Tab. 16

Alloy No.	Wt.-%			°C	
	Ag	Cu	Zn	Liquidus	Peritectic
154	—	10	90	570	422
155	2.5	7.5	90	550	424
156	5	5	90	530	426
157	7.5	2.5	90	515	428
158	10	—	90	501	430

17 The Zinc Corner

In order to establish this corner-diagram, the cooling curves as well as the quenching data were used, as a result of which we have got the one given in Fig. 19.

Fig. 19



The horizontal line AB refers to the peritectic reaction, $Liq. + \gamma \rightleftharpoons Liq. + \delta$, in the Cu-Zn system at 695° . The temperature of this reaction is depressed by the addition of silver from 695° to 620° , in accordance with which the curve BC makes its appearance to represent the ternary peritectical reaction. The horizontal line DT represents the binary peritectic reaction, $Liq. + \theta \rightleftharpoons \epsilon$, in the Ag-Zn system at 636° . The temperature is then depressed to 620° by the addition

of copper, the relation of which is traced by the curve DC . An alloy with 28% Ag, 65% Zn and 7% Cu, which is a point in the curve

DC , was quenched at 550° , the structure of which is $\gamma + \epsilon$, as shown in Photo 28. These two peritectical lines BC and DC meet at a point C with 26% Ag, 7% Cu and 67% Zn, which is the point of intersection of the peritectical line BCD and the curve BC connecting a point d in the 60% Zn and another d in the 65% Zn-section. The surface $ABCFA$ corresponds to the former reaction and the surface $CFTDC$ to the latter, while the surface $BGmcB$ is the liquidus of δ .

The horizontal line cG shows the peritectic reaction, $\text{Liq.} + \delta \rightleftharpoons \text{Liq.} + \epsilon$, in the Cu-Zn system at 590° , the temperature being raised to 596° with the increase in copper. The ternary peritectical line on the addition of silver is given by Gm , which fades away near the point of 22% Ag, 5% Cu and 73% Zn. This reaction is shown by the surface $cGmhc$, in which $cfohc$ is the solidus of the binary complex $\delta + \epsilon$ and $fGmof$ is the surface of the liquid which will solidify with the surface of $fpqof$ on the temperature being lowered.

The surface $AchFA$ is the solidus of the ternary δ which, being unstable, splits up on the one hand into γ on the surface $abdca$, and on the other into ϵ on the surface $cbdhc$. As to the field for the separation of γ from δ , an alloy with 6% Ag, 70% Zn and 24% Cu, quenched at 625° , becomes homogeneous ($=\delta$) as Photo 29 shows, but quenched at 565° it becomes heterogeneous ($=\delta + \gamma$) as Photo 30 shows. As to the separation of ϵ from δ , an alloy with 22% Ag, 65% Zn and 13% Cu, when quenched at 600° shows the δ -structure (Photo 26), but when quenched at 565° , it turns heterogeneous (Photo 27: $\delta + \epsilon$).

The horizontal line $a'f'$ shows the eutectoidal reaction, $\delta \rightleftharpoons \gamma + \epsilon$, in the Cu-Zn system at 555° the temperature being raised to 562° with the increase in silver as shown by the curve bd . Though the line $a'f'$ corresponds to a nonvariant reaction in the Cu-Zn system, the curve bd in the ternary system does not, there being only the three phases δ , γ and ϵ in equilibrium. The surface $a'f'nga'$ corresponds to the binary eutectoidal: the structure under the surface consists therefore of $\gamma + \epsilon$: see Photos 31 and 34. The surface $GRSDCmG$ is the liquidus of ϵ , and $fPqDCof$ is its solidus.

The horizontal line PR shows the binary peritectic reaction, $\text{Liq.} + \epsilon \rightleftharpoons \gamma$, in the Cu-Zn system at 423° , while the horizontal line qS shows the binary peritectic reaction, $\text{Liq.} + \epsilon \rightleftharpoons \gamma$, in the Ag-Zn system at 430° . The temperature of the former reaction is raised by the addition of silver, while that of the latter is lowered by the addition

of copper, so that both the ternary reactions will be united at the temperatures between 423° and 430° . These binary peritectic reactions going on in the ternary system are shown by the surface $PQSRP$. The equilibrium between three phases, ϵ , η and the melt, is shown by the curve RS . The alloys at the zinc corner limited by a line connecting 4% Ag in the Ag-Zn and 1.4% Cu in the Cu-Zn, must therefore form a homogeneous field (η). In so far as this is concerned, we come to have four parts there at room temperatures :

- 1) $a''f'D'T'a''$: structure, $\gamma + \epsilon$
- 2) $f''P'q'D'f''$: structure, ϵ
- 3) $P'q'S'R'P'$: structure, $\epsilon + \eta$
- 4) $R'S'K'$: structure, η

18 90% Ag-Section

The alloys, and the thermal data are given in Tab. 17 and the sectional diagram in Fig. 20.

Fig. 20

Tab. 17



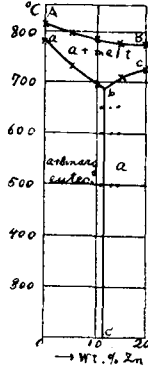
Alloy No.	Wt.-%			°C	
	Ag	Cu	Zn	Liquidus	Solidus
159	90	10	—	875	775
160	„	7.5	2.5	873	740
161	„	6	4	871	727
162	„	5	5	870	805
163	„	2.5	7.5	868	830
34	„	—	10	865	845

In this section there occurs crystallization, AB standing for the liquidus of the solid solution a , ab for the solidus of the binary eutectic $a + a$, and abc' for that of a .

19 80% Ag-Section

Alloys and thermal data, and the diagram are given in Tab. 18 and in Fig. 21.

Fig. 21



Tab. 18

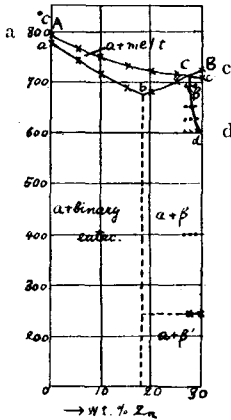
Alloy No.	Wt.-%			°C	
	Ag	Cu	Zn	Liquidus	Solidus
164	80	20	—	807	776
165	„	15	5	797	728
166	„	10	10	785	695
167	„	5	15	777	712
16	„	—	20	772	725

Exactly the same explanation applies here as in the previous section.

20 70% Ag-Section

The alloys and the thermal data are given in Tab. 19 and the diagram, in Fig. 22.

Fig. 22



Tab. 19

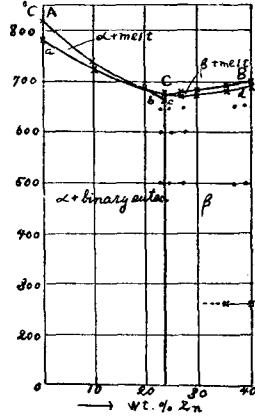
Alloy No.	Wt.-%			°C			
	Ag	Cu	Zn	Liquidus	Solidus	Peritectic	Transformation
168	70	30	—	785	777	—	—
169	„	25	5	760	740	—	—
12	„	20	10	740	714	—	—
170	„	15	15	726	—	688	—
31	„	10	20	720	—	680	—
171	„	5	25	712	—	700	—
172	„	2	28	710	707	—	240
49	„	—	30	709	705	—	242

AC is the liquidus of a , BC that of β , ab the solidus for the binary eutectic $a + a$, Cc that for β , and bC that for the binary complex $a + \beta$. The curve Cd shows the segregation of a from β .

21 60% Ag-Section

The alloys and thermal data are given in Tab. 20 and the diagram in Fig. 23.

Fig. 23



Tab. 20

Alloy No.	Wt.-%			°C		
	Ag	Cu	Zn	Liquidus	Solidus	Transformation
173	60	40	—	815	776	—
10	„	30	10	735	725	—
27	„	20	20	681	680	—
174	„	17	23	672	670	—
175	„	13	27	675	671	—
47	„	10	30	680	675	—
58	„	5	35	689	681	262
69	„	—	40	695	685	260

The liquidus is represented by $AbCB$, in which Abc is for α , and BC for β . The solidus consists of two branches, of which abc is for the binary eutectic $\alpha + a$ and cd for β . At the point b there are three phases in equilibrium, i. e. α , β and the melt, just as described in connection with the 20% Zn-section.

22 50% Ag and 40% Ag-Sections

The compositions of the alloys and the thermal data of these two sections are given in Tables 21, and 22.

Tab. 21

Alloy No.	Wt.-%			°C	
	Ag	Cu	Zn	Liquidus	Solidus
176	50	50	—	851	776
9	„	40	10	795	727
25	„	30	20	742	688
177	„	25	25	703	673
46	„	20	30	684	675
57	„	15	35	684	675
67	„	10	40	684	678
76	„	5	45	678	672
85	„	—	50	668	656

Tab. 22

Alloy No.	Wt.-%			°C		
	Ag	Cu	Zn	Liquidus	Solidus	Peritectic
178	40	60	—	887	776	—
8	„	50	10	845	728	—
24	„	40	20	790	684	—
179	„	32	28	735	—	—
45	„	30	30	725	722	—
56	„	25	35	710	700	—
66	„	20	40	705	697	—
75	„	15	45	697	687	—
84	„	10	50	681	673	—
94	„	5	55	662	630	—
180	„	2	58	645	—	635
109	„	—	60	637	—	636

The sectional diagrams. Fig. 24 and 25, are drawn on the basis of these data.

Fig. 24

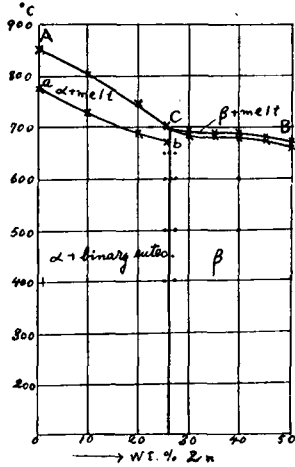
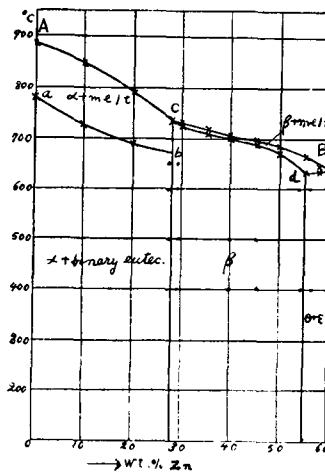


Fig. 25

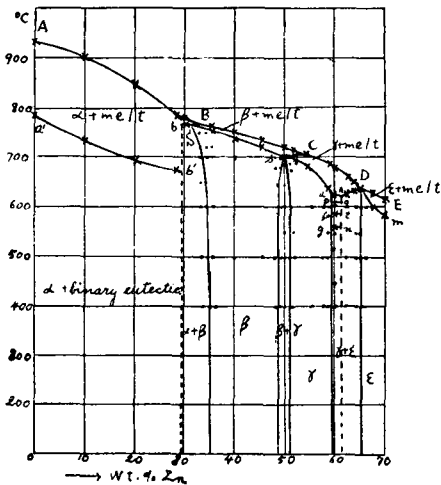


The same explanation applies here as given in the previous section except only that there is a new, curve dB in the 40% Zn-section, along which ϵ is separated, due to the binary peritectic reaction, $Liq. + \theta \rightleftharpoons \epsilon$, in the Ag-Zn system.

23 30% Ag-Section

The alloys and the thermal data are given in Tab. 23 and the diagram in Fig. 26.

Fig. 26



The liquidus consists of four branches, of which AB is for α , BC for β , CD for γ , and DE for ϵ . The solidus consists also of several branches, of which ab' is for the solidification of the binary eutectic $\alpha + a$, bs for that of the binary complex $\alpha + \beta$ due to the binary peritectic reaction, $Liq. + a \rightleftharpoons \beta$, in the Cu-Zn system, Ss for β , sd for γ , Pq for δ , and hd for the binary peritectic reaction, $Liq. + \theta \rightleftharpoons \epsilon$, in the Ag-Zn system. Along sC , γ is separated due to the binary

Tab. 23

Alloy No.	Wt.-%			°C				
	Ag	Cu	Zn	Liquidus	Solidus	Peritectic	Separation of ϵ from δ	Eutectoidal transformation
181	30	70	—	934	776	—	—	—
7	„	60	10	999	734	—	—	—
23	„	50	20	844	689	—	—	—
182	„	42	28	785	673	—	—	—
43	„	40	30	780	—	765	—	—
183	„	38	32	767	—	765	—	—
55	„	35	35	760	751	—	—	—
65	„	30	40	749	739	—	—	—
74	„	25	45	733	724	—	—	—
83	„	20	50	716	—	705	—	—
184	„	18	52	710	702	704	—	—
93	„	15	55	703	680	—	—	—
185	„	11	59	682	645	—	—	—
106	„	10	60	675	610	623	590 ?	562 ?
186	„	7	63	650	—	625	—	—
187	„	6	64	647	—	632	—	—
120	„	5	65	630	627	—	—	—
188	„	3	67	629	600	—	—	—
134	„	—	70	619	583	—	—	—

peritectic reaction, $Liq. + \beta \rightleftharpoons Liq. + \gamma$. Along gn , the binary complex $\gamma + \epsilon$ is separated due to the binary eutectoidal transformation in the Cu-Zn system. Lastly, γ is separated from δ along the curve ft .

24 20% Ag and 10% Ag-Sections

The compositions of the alloys and the thermal data of these two sections are given in Tables 24 and 25.

The sectional diagrams, Figs. 27 and 28, are drawn on the basis of these data.

These two sections differ from the 30% Ag-section in the following

Tab. 24

Alloy No.	Wt.-%			°C					
	Ag	Cu	Zn	Liquidus	Solidus	Peritectic 1	Peritectic 2	Separation of δ or ϵ from δ	Eutectoidal transformation
189	20	80	—	970	777	—	—	—	—
6	"	70	10	948	735	—	—	—	—
22	"	60	20	900	693	—	—	—	—
39	"	50	30	835	674	—	—	—	—
190	"	48	32	824	—	810	—	—	—
191	"	47	33	817	—	808	—	—	—
54	"	45	35	808	800	—	—	—	—
64	"	40	40	797	788	—	—	—	—
73	"	35	45	785	777	—	—	—	—
82	"	30	50	772	756	—	—	—	—
192	"	28	52	762	749	751	—	—	—
193	"	26	54	752	740	748	—	—	—
91	"	25	55	750	735	745	—	—	—
102	"	20	60	729	705	—	—	—	—
194	"	16	64	700	635	638	—	585	560
114	"	15	65	694	627	640	—	570?	561
195	"	13.5	66.5	680	610	640	—	588	560
196	"	13	67	675	—	636	595	—	561
130	"	10	70	637	—	—	594	—	—
141	"	5	75	592	570	—	—	—	—
148	"	—	80	570	435	—	—	—	—

Tab. 25

Alloy No.	Wt.-%			°C					
	Ag	Cu	Zn	Liquidus	Solidus	Peritectic 1	Peritectic 2	Separation of ϵ or γ from δ	Eutectoidal transformation
197	10	90	—	1028	777	—	—	—	—
5	"	80	10	999	734	—	—	—	—
21	"	70	20	952	692	—	—	—	—
38	"	60	30	896	676	—	—	—	—
198	"	59	31	886	673	—	—	—	—
199	"	57	33	872	—	853	—	—	—
52	"	55	35	860	—	850	—	—	—
63	"	50	40	849	842	—	—	—	—
72	"	45	45	837	827	—	—	—	—
81	"	40	50	820	805	—	—	—	—
200	"	36	54	805	—	791	—	—	—
89	"	35	55	800	783	790	—	—	—
201	"	33	57	795	785	—	—	—	—
101	"	30	60	785	770	—	—	—	—
112	"	25	65	768	730	—	—	—	—
202	"	23	67	750	665	674	—	590	557
203	"	22	68	742	650	674	—	580	556
126	"	20	70	730	625	674	—	570	557
204	"	19	71	715	—	675	595	565	558
205	"	17	73	690	—	674	595	—	558
139	"	15	75	675	593	672	595	—	—
146	"	10	80	610	585	—	596	—	—
152	"	5	85	557	—	428	—	—	—
158	"	—	90	501	—	430	—	—	—

points:— δ is solidified along de , γ separated from δ along ft , ϵ separated from δ along et , the binary complex $\gamma+\epsilon$ separated along

Fig. 27

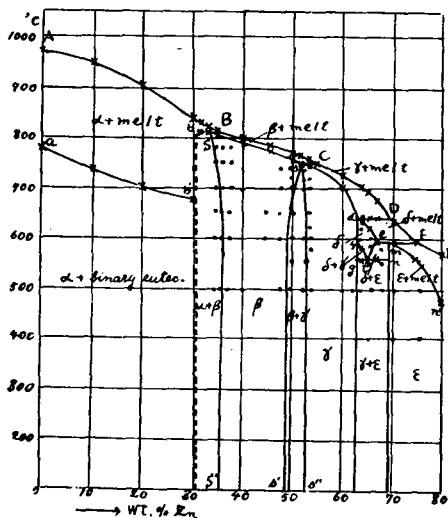
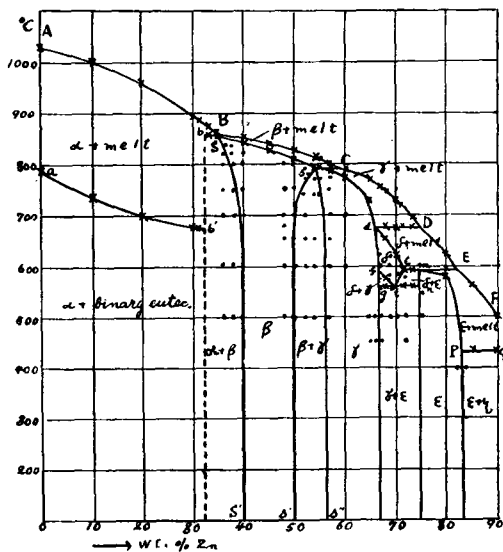


Fig. 28

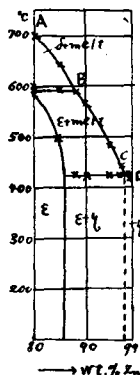


gh due to the reaction, $\delta \rightleftharpoons \gamma + \epsilon$, in the Cu-Zn system, and, lastly, ϵ separated along *eE* due to the binary peritectic reaction, $\text{Liq.} + \delta \rightleftharpoons \text{Liq.} + \epsilon$, in the Cu-Zn system. The difference between the 10% Ag and the 20% Ag-section is, that a new curve *Pq* appears here, which corresponds to the binary peritectic reaction: $\text{Liq.} + \epsilon \rightleftharpoons \gamma$.

25 A Part of 1% Ag-Section

Finally, a part of 1% Ag-section was investigated in order to find out the relation of η in equilibrium. The alloys and the thermal data,

Fig. 29



Tab. 26

Alloy No.	Wt.-%			C°		
	Ag	Cu	Zn	Liquidus	Solidus	Peritectic
206	1	19	80	697	580	590
207	"	14	85	640	480	591
208	"	11	88	590	—	423
209	"	9	90	565	—	423
210	"	4	95	482	—	424
211	"	2	97	440	—	425
212	"	1	98	425	424	—
213	"	—	99	425	419	—

and the diagram are given in Tab. 26 and Fig. 29.

The curve CD is the liquidus and Ce the solidus of η . At the point C , three phases ϵ , η and the melt, are in equilibrium.

Tab. 27

Wt.-% Zn	°C			Peritectic Crystallization in Sec.	°C Transformation	Transformation in Sec.
	Liquidus	Solidus	Peritectic			
10	865	845	—	—	—	—
15	822	780	—	—	—	—
20	772	725	—	—	—	—
22	760	—	710	20	—	—
25	730	—	710	60	240	10
27	715	—	709	80	241	20
30	709	705	—	—	242	70
35	705	700	—	—	240	150
36	703	700	—	—	240	160
38	700	697	—	—	250	130
40	695	685	—	—	260	120
42	689	686	—	—	263	150
43	687	684	—	—	262	100
45	679	670	—	—	261	100
47	668	665	—	—	—	—
50	668	656	—	—	—	—
55	655	—	635	20	—	—
58	647	—	636	60	—	—
60	637	—	636	100	—	—
65	633	611	—	—	—	—
70	619	583	—	—	—	—
75	597	536	—	—	—	—
80	570	435	—	—	—	—
83	555	—	430	20	—	—
85	544	—	431	50	320?	—
90	501	—	430	90	320	—
95	447	425	430	30	320	—
97	430	420	—	—	320?	—
99	425	419	—	—	—	—

28 The Complete Equilibrium-Diagram

With all the data above given, we were able to draw the iso-thermal (Fig. 30), the spatial (Fig. 31), and the projection diagram (Fig. 32).

Fig. 30

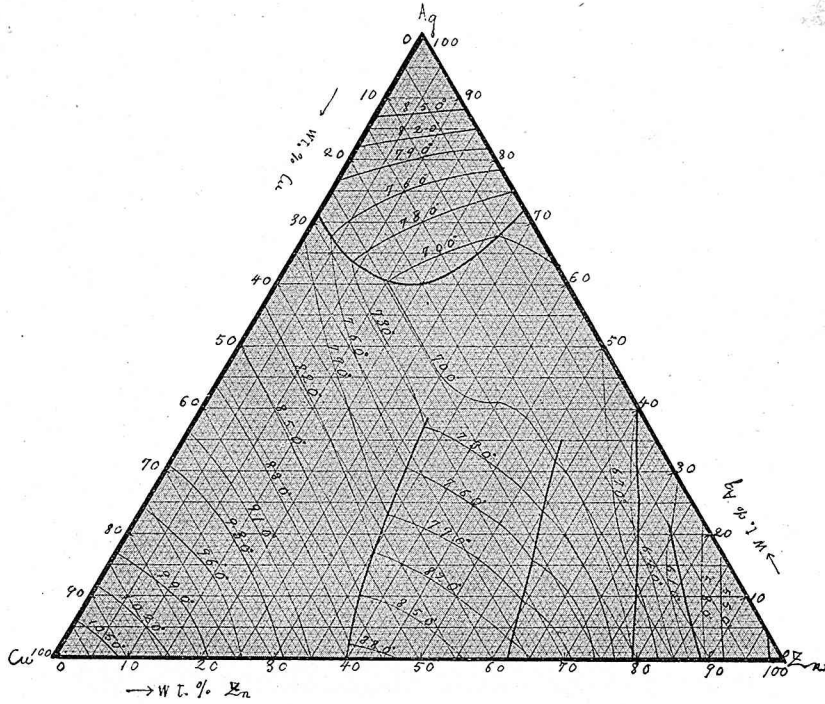


Fig. 31

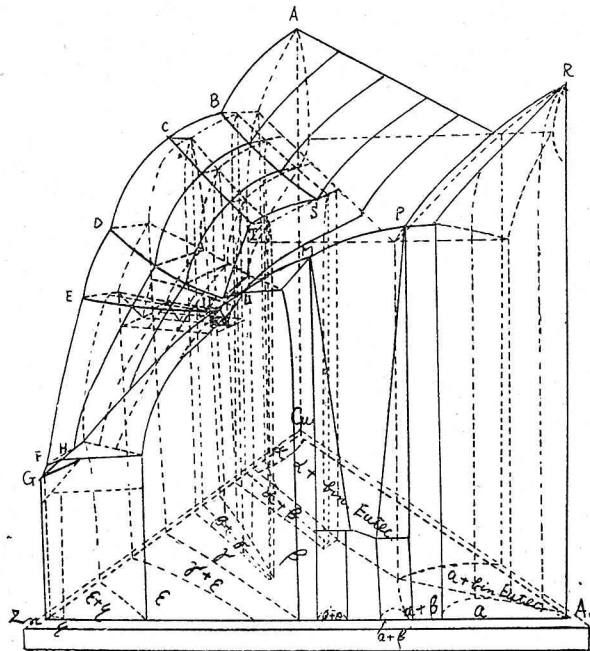
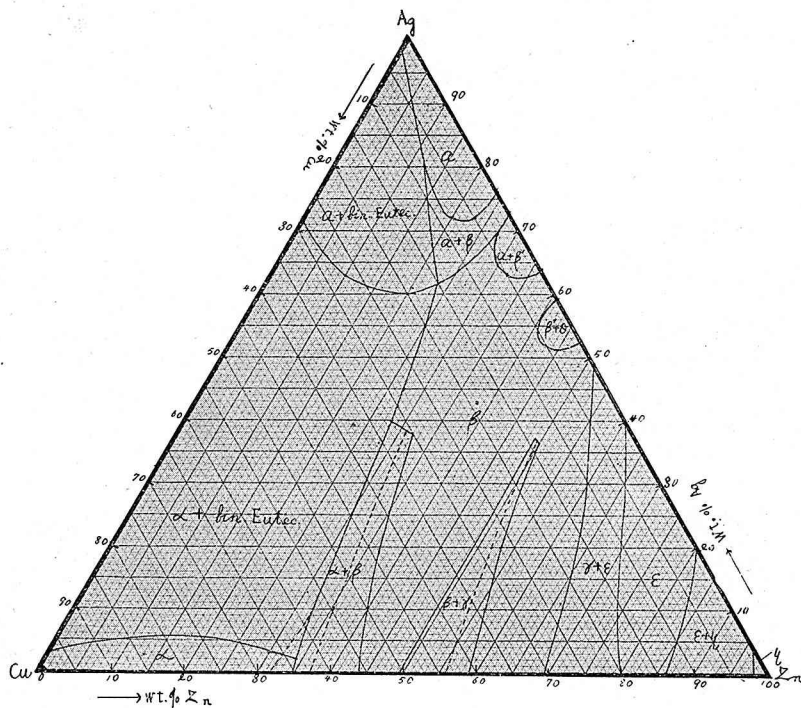


Fig. 32



In Fig. 32, the full lines refer to the field boundaries at ordinary temperatures, while the dotted lines refer to those at higher temperatures.

In conclusion, the author desires to express his indebtedness to Prof. Dr. M. Chikashige for his kind guidance and valuable advice during the course of the investigation.

Institute for Chemical Research,
Imperial University, Kyoto.

Shûzô Ueno

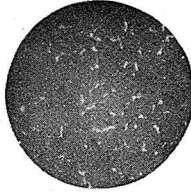


Photo 1. 10%Ag, 10%Zn and 80%Cu, $\times 150$.

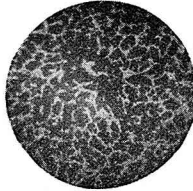


Photo 2. 50%Ag, 10%Zn and 40%Cu $\times 150$.

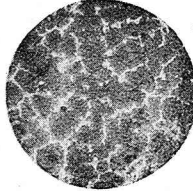


Photo 3. 10%Ag, 17%Zn and 73%Cu, $\times 150$.

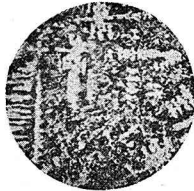


Photo 4. 80%Ag, 10%Zn and 10%Cu, $\times 150$.



Photo 5. 3%Ag, 10%Zn and 87%Cu, Annealed at 600° for two days, $\times 150$.



Photo 6. 6%Ag, 10%Zn and 84%Cu, Annealed at 700°, $\times 150$.

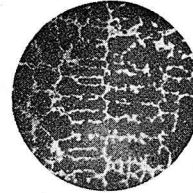


Photo 7. 20%Ag, 50%Zn and 60%Cu, $\times 150$.

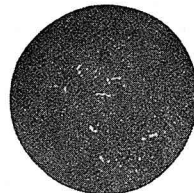


Photo 8. 6%Ag, 20%Zn and 74%Cu, Quenched at 600°, $\times 150$.



Photo 9. 87%Ag, 10%Zn and 3%Cu, Annealed at 500° for 1 day, $\times 150$.

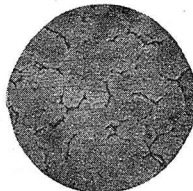


Photo 10. 70%Ag, 20%Zn and 10%Cu, $\times 150$.

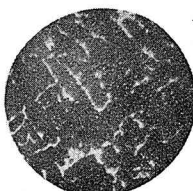


Photo 11. 20%Ag, 30%Zn and 50%Cu, $\times 150$.

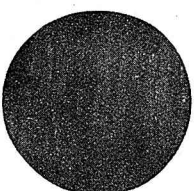


Photo 12. 30%Ag, 40%Zn and 30%Cu, $\times 150$.



Photo 13. 5%Ag, 40%Zn and 55%Cu, Quenched at 600° after being kept at that temperature for a few minutes, $\times 150$.

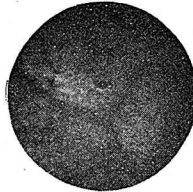


Photo 14. The same alloy quenched at 820° after being kept at that temperature for a few minutes, $\times 150$.

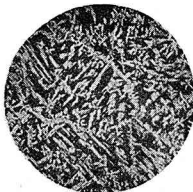


Photo 15. 10%Ag, 40%Zn and 50%Cu, $\times 150$.



Photo 16. 45%Zn, 3%Ag and 52%Cu, Quenched at 400° after being kept at that temperature for 30° minutes, $\times 150$.

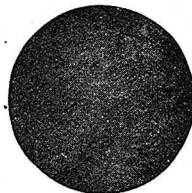


Photo 17. 4%Zn, 3%Cu and 5%Ag, Quenched at 650° after being kept at that temperature for 30 minutes, $\times 150$.

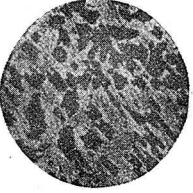


Photo 18. 1%Ag, 33%Zn and 52%Cu, $\times 150$.

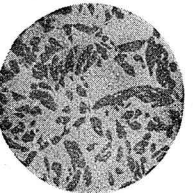


Photo 19. 50%Zn, 20%Ag and 30%Cu, Quenched at 600° after being kept at that temperature for 30 minutes, $\times 150$.

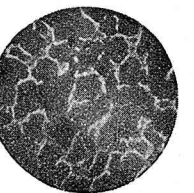


Photo 20. 3%Ag, 55%Zn and 42%Cu, Quenched at 600° after being kept at that temperature for 30 minutes, $\times 150$.

Shūzō Ueno

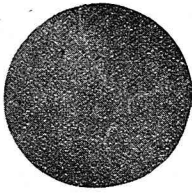


Photo 21. The same alloy quenched at 820° after being kept at that temperature for 30 minutes, ×150.



Photo 22. 30%Ag, 50%Zn and 20%Cu, ×150.

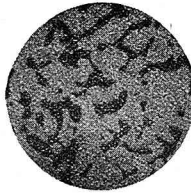


Photo 23. 5%Cu, 55%Zn and 4%Ag, ×150.



Photo 24. 16%Ag, 67%Zn and 19%Cu. Quenched at 610° after being kept at that temperature for 30 minutes, ×150.

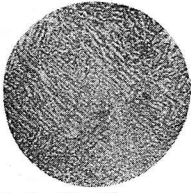


Photo 25. The same alloy quenched at 500° after being kept at that temperature for 30 minutes, ×150.

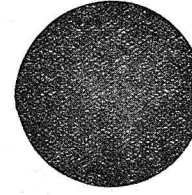


Photo 26. 22%Ag, 65%Zn and 13%Cu. Quenched at that temperature for 30 minutes, ×150.

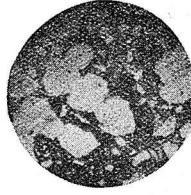


Photo 27. The same alloy quenched at 565° after being kept at that temperature for 30 minutes, ×150.

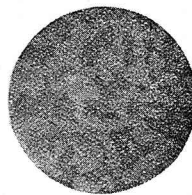


Photo 28. 28%Ag, 65%Zn and 7%Cu. Quenched at 550°, ×150.

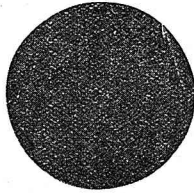


Photo 29. 6%Ag, 70%Zn and 24%Cu. Quenched at 625° after being kept at that temperature for 30 minutes, ×150.

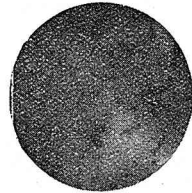


Photo 30. The same alloy quenched at 565° after being kept at that temperature for 30 minutes, ×150.



Photo 31. The same alloy quenched at 500° after being kept at that temperature for 30 minutes, ×150.

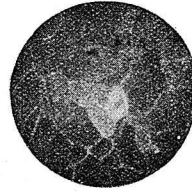


Photo 32. 11%Ag, 70%Zn and 19%Cu. Quenched at 585° after being kept at that temperature for 30 minutes, ×150.



Photo 33. The same alloy quenched at 600° after being kept at that temperature for 30 minutes, ×150.



Photo 34. The same alloy quenched at 500° after being kept at that temperature for 30 minutes, ×150.

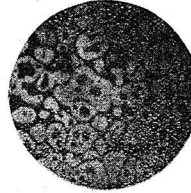


Photo 35. 5%Ag, 84%Zn and 11%Cu. Quenched at 530°, ×150.



Photo 36. 90%Zn, 5%Ag and 5%Cu, ×150.

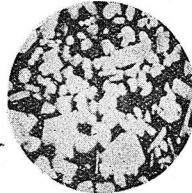


Photo 37. 1%Ag, 4%Cu and 95%Zn, ×150.

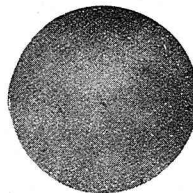


Photo 38. 0.2%Cu, 99%Zn and 0.7%Ag, ×150.

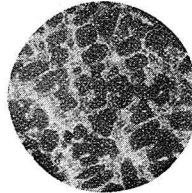


Photo 39. 16%Ag, 65%Zn and 19%Cu. Quenched at 580° after being kept at that temperature for a few minutes, ×150.